

Accepted Manuscript

Title: Heterogeneous catalysts hold the edge over homogeneous systems: Zeolite-Y encapsulated complexes for Baeyer-Villiger oxidation of cyclohexanone

Author: Jignasu P. Mehta Digvijaysinh K. Parmar Dinesh R. Godhani Haresh D. Nakum Nisheeth C. Desai



PII: S1381-1169(16)30187-X
DOI: <http://dx.doi.org/doi:10.1016/j.molcata.2016.05.016>
Reference: MOLCAA 9891

To appear in: *Journal of Molecular Catalysis A: Chemical*

Received date: 30-1-2016
Revised date: 10-5-2016
Accepted date: 13-5-2016

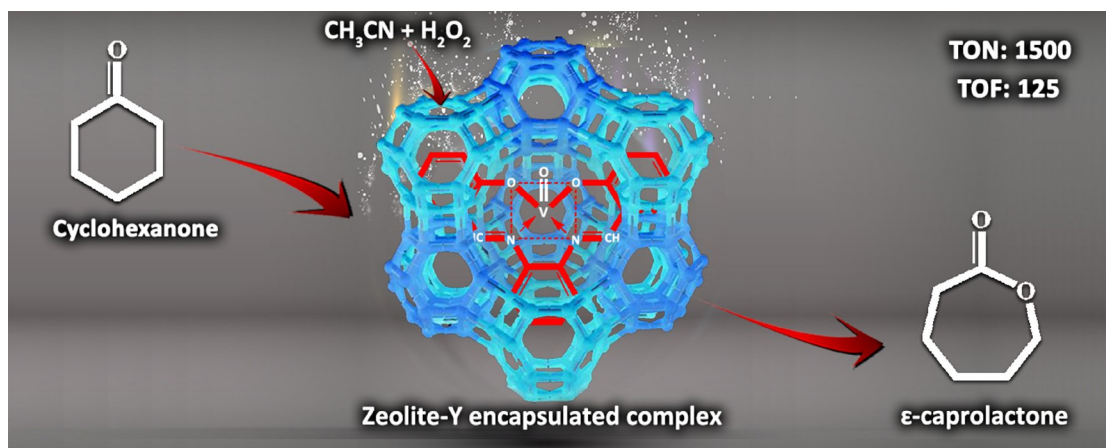
Please cite this article as: Jignasu P.Mehta, Digvijaysinh K.Parmar, Dinesh R.Godhani, Haresh D.Nakum, Nisheeth C.Desai, Heterogeneous catalysts hold the edge over homogeneous systems: Zeolite-Y encapsulated complexes for Baeyer-Villiger oxidation of cyclohexanone, Journal of Molecular Catalysis A: Chemical <http://dx.doi.org/10.1016/j.molcata.2016.05.016>

This is a PDF file of an unedited manuscript that has been accepted for publication. As a service to our customers we are providing this early version of the manuscript. The manuscript will undergo copyediting, typesetting, and review of the resulting proof before it is published in its final form. Please note that during the production process errors may be discovered which could affect the content, and all legal disclaimers that apply to the journal pertain.

HIGHLIGHTS:

- ✚ Heterogenization of M(II/IV) complexes within zeolite-Y by Flexible-Ligand method.
- ✚ Characterization of synthesized materials with ICP-OES, BET, XRD, IR, UV-Vis, TGA.
- ✚ B-V oxidation of cyclohexanone over neat and zeolite-Y encapsulated complexes.
- ✚ The effect of reaction parameters on substrate conversion was also tested.
- ✚ [VO(pamp)]-Y exhibited eventual performance by providing 1500 TONs.

GRAPHICAL ABSTRACT:



Heterogeneous catalysts hold the edge over homogeneous systems: Zeolite-Y encapsulated complexes for Baeyer-Villiger oxidation of cyclohexanone

Jignasu P. Mehta*, Digvijaysinh K. Parmar, Dinesh R. Godhani, Haresh D. Nakum and Nisheeth C. Desai

Department of Chemistry, (UGC NON-SAP & DST-FIST sponsored Department) Mahatma Gandhi Campus, Maharaja Krishnakumarsinhji Bhavnagar University, Bhavnagar 364 002, Gujarat, India

ABSTRACT

A series of heterogeneous catalysts [M(pamp)]-Y (Where, M = V, Mn, Fe or Cu; pamp = 2,2'-((1E,1'E)-(1,2-phenylenebis(azanylylidene))bis(methanylylidene))diphenol) was prepared by encapsulation of metal complexes within zeolite-Y. Synthesized materials were characterized by chemical, BET and thermogravimetric (TG) analysis, X-ray diffraction (XRD), UV-vis and infrared spectroscopies, and scanning electron microscopy (SEM). Zeolite-Y encapsulated complexes were tested in Baeyer-Villiger (B-V) oxidation of cyclohexanone beside neat complexes to check the aptitude of heterogeneous catalysis over the homogeneous system. The effect of experimental variables viz., solvents, catalysts amount, the mole ratio of substrate to an oxidant, temperature and reaction time on substrate conversion was also tested. Under the optimized reaction conditions, [VO(pamp)]-Y was found to be a potential candidate by providing 1500 TONs in cyclohexanone oxidation, and the selectivity towards ϵ -caprolactone was 85.2%.

Keywords: Heterogeneous catalysts; Zeolite-Y encapsulated complexes; Baeyer-Villiger oxidation; Cyclohexanone

*Corresponding author: Jignasu P. Mehta

Corresponding Author's address

Department of Chemistry, (UGC NON-SAP & DST-FIST sponsored department) Mahatma Gandhi Campus, Maharaja Krishnakumarsinhji Bhavnagar University, Bhavnagar 364 002, Gujarat, India

E-mail: jpm1569@yahoo.co.in (M) 09408706147

1. Introduction

The Baeyer-Villiger (B-V) oxidation, which could freely transform ketones to lactones or esters, is of marked synthetic value and has been extensively used in various syntheses of fine chemicals, pharmaceuticals and monomers for polymerization [1-7]. Usually, B-V oxidation with peracids, like trifluoroperacetic acid [8], perbenzoic acid [9] and m-chloroperbenzoic acid [10] eventually produce large amount of waste. In last few years, a wide range of homogeneous metal complexes have been used for B-V oxidation [11-13] to improve reaction rate and selectivity, since their acid-base and redox properties can be tuned easily by simply changing ligand composition. However, homogeneous systems are often regarded as ill-defined with many limitations, including the decomposition and deactivation due to the formation of dimeric μ -oxo- and peroxy- bridged species, and separation problem as well.

On the other end, heterogeneous systems lights up the catalysis field with sparkling rewards as catalyst separation from the homogeneous systems is typically stropopy. Plentiful efforts have been made to incorporate homogeneous Schiff base complexes on solid supports, such as anchoring metal complexes in a polymeric matrix [14], sulfonic acid-functionalized mesoporous SBA-15 [15], and encapsulation in zeolite cavities [16-19] have also been reported. In specific, encapsulation of metal complexes in the nanopores of zeolite-Y is an eye-catching eco-friendly technique for heterogenization; since no leaching is perceived when the complex is confined entirely in the nanocavity of zeolite-Y [20-23]. The as-prepared hybrid inorganic-organic material holds the number of heterogeneous catalysis feature over homogeneous catalysts in this context viz., shape selectivity, site isolation, better reactivity, withstand high temperatures, be prepared with the desired texture, be recycled, and be reused [24-28]. It has been prominent that the space constraints forced by the host framework can have a weighty impact on the geometry of the guest complex, which can induce changes in magnetic, spectroscopic and redox properties of the encapsulated complex, leading to a boosted activity and selectivity rather than its outlook in homogeneous account [29-31]. Zeolite-Y encapsulated complexes have been shown to be potential heterogeneous catalysts for numerous reaction processes viz., oxidation of alkanes [32], alkenes [33,34], alcohols [35,36], olefins [37], and ketones [38], with certain oxidants,

viz., tert-butylhydroperoxide (TBHP) [34], hydrogen peroxide (H_2O_2) [35], and molecular oxygen (O_2) [39].

So, there is still an attention in catalytic systems able to perform B-V reaction in a more environmentally friendly way, using innocuous oxidants, solvents, and reagents. The use of heterogeneous catalyst and hydrogen peroxide allows a clean oxidation as the catalyst can be easily removed and reused. Hydrogen peroxide is the ideal oxidant in zeolite systems, as it is extremely mobile in the zeolitic pores due to a smaller size. Additionally, it is inexpensive and environmentally-friendly to be used on a commercial scale. Although, aerobic oxidation is likely to proceed at a slower rate due to the incompetence of molecular oxygen to be initiated as compared to very reactive species like peroxides. However, zeolite-Y encapsulated complexes have not been mainly focused on catalysts in the B-V oxidation reaction, thus received only limited attention [38]. Therefore, with the purpose of choosing a cleaner system for B-V oxidation, here, zeolite-Y encapsulated complexes were used as a heterogeneous catalyst for the liquid-phase oxidation of cyclohexanone with 30% H_2O_2 as an oxidizing agent.

2. Materials and Methods

2.1. Materials and physical measurements

The zeolite-Y ($\text{Si/Al} = 2.60$) was purchased from Hi-media (India). 2-hydroxybenzaldehyde, o-phenylenediamine, 30% hydrogen peroxide (H_2O_2) and cyclohexanone were purchased from Aldrich. Transition metal salts and solvents were purchased from Merck and were used as received.

To ensure the encapsulation of complex and preservation of the zeolite framework after the formation of the metal complex inside the cavity of zeolite-Y, synthesized materials were characterized by various physico-chemical techniques. ICP-OES (Model: PerkinElmer optima 2000 DV) was carried out to determine the composition of Si, Al, Na, V, Mn, Fe, and Cu metal ions. The elemental analysis (C, H, N) of the synthesized materials was carried out on Perkin Elmer, USA 2400-II CHN analyzer. The specific surface area and pore volume were measured by a multipoint BET method using ASAP 2010, micrometrics surface area analyzer. The X-ray diffractograms of the solids were recorded on a Bruker AXS D_8 Advance X-ray powder diffractometer with a Cu K_α radiation as the incident beam to confirm the

crystallinity of zeolite-Y encapsulated complexes. The scanning electron micrographs of the zeolite-Y encapsulated VO(IV) complex were recorded using a SEM instrument (Model: LEO 1430 VP). The sample materials were coated with a thin film of gold before recording the SEM to shield the material surface from thermal damage by the electron beam. Infrared spectra were recorded in the 4000-400 cm^{-1} range on a Thermo Nicolet IR200 FT-IR spectrometer in KBr. UV-vis spectra were recorded in the range of 200-800 nm on a UV-1800 Spectrophotometer, Shimadzu. Thermogravimetric (TG) analysis was performed using a thermal gravimetric analysis instrument (Shimadzu TGA-50H) with a flow rate of 20.0 mL min^{-1} and a heating rate of 10 $^{\circ}\text{C min}^{-1}$. Products of the catalytic oxidation reactions were identified using GC-MS having a BP-5 capillary column (30m \times 0.25mm \times 0.25 μm) 95% silicoxane surface and FID detector. The reaction products were confirmed by GC-MS model Shimadzu, QP-2012.

2.2. Synthesis of Schiff base ligand 'pamp'

Schiff base ligand pamp (2,2'-((1E,1'E)-(1,2-phenylenebis(azanylylidene))bis(methanylylidene))diphenol) was synthesized by stirring a mixture of 2-hydroxybenzaldehyde (2.10 mL, 0.02 mole) with o-phenylenediamine (1.08 g, 0.01 mole) in 50 mL of ethanolic medium. The solid product was filtered and recrystallized from ethanol [40].

2.3. Synthesis of neat complexes [M(pamp)]

The solution of transition metal salts M(II/IV) (Where, M = $\text{VOSO}_4 \cdot 5\text{H}_2\text{O}$ / $\text{MnSO}_4 \cdot \text{H}_2\text{O}$ / $\text{FeSO}_4 \cdot 7\text{H}_2\text{O}$ / $\text{CuSO}_4 \cdot 5\text{H}_2\text{O}$) of 0.01 mole in 25 mL of deionized water was added to a 25 mL of an ethanolic solution of 0.01 mole ligand pamp, and the resulting solution was heated under reflux with constant stirring at 80 $^{\circ}\text{C}$ for 4-5 h. The pH of the solution was adjusted 5-6 by drop wise addition of an ethanolic solution of sodium acetate in it. The complexes were precipitated and was separated by filtration.

2.4. Synthesis of metal exchanged zeolite-Y [M(II/IV)-Y]

An amount of 4.0 g of zeolite-Y was suspended in 200 mL deionized water containing 0.012 M transition metal salt M(II/IV). The mixture was then heated to 100 $^{\circ}\text{C}$ with constant stirring for 24 h. The solid was filtered, washed with hot deionized water till the filtrate was free from any metal ion content, and dried for 6 h at 150 $^{\circ}\text{C}$ in a muffle furnace.

2.5. Synthesis of zeolite-Y encapsulated complexes [M(pamp)]-Y

Flexible ligand (FL) method [41] was used to prepare zeolite-Y encapsulated complexes. Typically a 1.0 g of activated metal exchanged zeolite-Y was added to an excessive amount of ligand pamp in 1,4-dioxane (50 mL). The mixture was then heated for 24 h with constant stirring under reflux condition on an oil bath. The resulting solid was treated for Soxhlet extraction with 1,4-dioxane, and acetonitrile to remove unreacted ligand, as well as metal complexes adsorbed on the peripheral surface of the zeolite-Y. Then the material was treated with aqueous 0.01 M NaCl to remove uncoordinated metal ions. Subsequently, it was washed with deionized water to remove any chloride ions present, and dried at 120 °C for 12 h. Chemical composition and IR stretching frequencies of ligand, neat complexes and zeolite-Y encapsulated complexes are given in Tables 1 & 2.

2.6. B-V oxidation of cyclohexanone

The B-V oxidation of cyclohexanone was tested to perceive the effect of heterogeneous catalysts over homogeneous stuff. The catalytic reactions were carried out in a two-necked 50 mL round bottomed flask. Reaction conditions for the liquid-phase oxidation of cyclohexanone were optimized as follows: cyclohexanone (1.03 mL, 0.01 mole), 30% H₂O₂ (2.06 mL, 0.02 mole) and catalyst (30 mg) were mixed in acetonitrile (5 mL). The resulting mixture was then refluxed at 80 °C in an oil-bath for 12 h with continuous stirring. After filtration and washing with a solvent, the filtrate was subjected to GC-MS to analyze and identify the reaction products.

3. Results and Discussion

3.1 Synthesis of catalysts

Synthesis of metal complexes [M(pamp)] (M = VO(IV), Mn(II), Fe(II), and Cu(II)) encapsulated in the nanocavity of zeolite-Y involved the exchange of transition metal(II) ions with sodium form of zeolite-Y followed by reaction of metal-exchanged zeolite-Y (M(II)-Y) with ligand pamp, where ligand move into the nanocavity of zeolite-Y due to its flexible nature and interacted with previously exchanged metal ions. It is expected that the [M(pamp)] complexes will be formed in the nanocavity as well as on the surface of the zeolite-Y. As the complex is neutral only a van der Waals interaction is active there to grip

the complex on the surface of the zeolite-Y. The resulted materials were subjected to Soxhlet extraction in 1,4-dioxane to remove excess ligand that remained uncoordinated in the nanocavities as well as situated on the exterior surface of the zeolite alongside free [M(pamp)]. The uncomplexed M(II) ions from the zeolite was removed by exchanging back [M(pamp)]-Y with aqueous 0.01 M NaCl solution. Therefore, presence of transition metal assessed by elemental analysis is correspond to the encapsulated complex. The resulted materials were further characterized by SEM, XRD, IR, UV-vis, and TGA. All these studies further supported the encapsulation of [M(pamp)] inside the nanocavities of zeolite-Y. Neat [M(pamp)] complexes have also been prepared for comparing its physico-chemical and catalytic properties with the encapsulated one. The FL method (scheme 1) leads to the encapsulation of VO(IV), Mn(II), Fe(II), and Cu(II) complexes of pamp ligand inside the nanocavities of zeolite-Y.

3.2 Catalysts characterizations

3.2.1 The chemical analysis data

The analytical data of synthesized materials were performed and summarized in Table 1. Neat complexes derived from ligand pamp are formed by coordination of metal and ligand in 1:1 molar ratio. The chemical analysis of the zeolite-Y encapsulated complexes reveals the presence of organic matter with a C/N ratio almost similar to that of neat complexes. As well as, Si and Al contents in the zeolite-Y encapsulated complexes and parent zeolite-Y are nearly in the same ratio. This specifies a slight variation in the zeolite framework is not due to the dealumination during encapsulation. Moreover, the concentration of metal ion in the encapsulated complexes is found to be reduced than the metal exchanged zeolite-Y, which leads to the fact of metal leaching during the encapsulation process. Therefore, only small amount of complex could be there inside the cavities of zeolite-Y.

3.2.2 Specific surface area and pore volume studies

Specific surface area and pore volume values measured by nitrogen adsorption isotherms at relative pressures (p/p_0). As tabulated in Table 3, the results of the surface area and pore volume data showed a considerable decrease in zeolite-Y encapsulated complexes

than that of parent zeolite-Y, which is the sign to prove the internal location of encapsulated complexes [42]. However, the zeolite framework is not affected by the encapsulation as verified by the XRD pattern.

3.2.3 Powder X-ray diffraction study

The X-ray diffraction (XRD) patterns of synthesized materials were recorded to ensure the encapsulation of complexes inside the cavities of zeolite-Y (see supplementary data). The encapsulated complexes show similar peaks to those of zeolite Y; except for a minor variation in the intensity of the peaks, no new crystalline pattern appears. These facts verify that the framework and crystallinity of zeolite were unspoiled during the encapsulation and that the complexes were well-defined in the cages. The peak intensities of the 2 2 0 and 3 1 1 reflections have been supposed to be associated with the sites of cations. In zeolite Y, the order of peak intensity is in the order: $I_{220} > I_{311}$, while in M(II/IV)-Y and [M(pamp)]-Y, the order of peak intensity became $I_{311} > I_{220}$. This intensity reversal has previously been identified and empirically associated with the existence of a large complex within the cavity of zeolite-Y [43,44], which may be associated with the rearrangement of randomly coordinated free cations during complex formation [45]. The above observations clearly indicate the unspoiled crystallinity of the zeolite-Y framework during the metal exchange and encapsulation process as well. These results also state that the cavities are capable enough to keep these complexes without any loss in crystallinity of the zeolite-Y.

3.2.4 Scanning electron microscopic (SEM) study

Basically, the formation of metal complexes was targeted inside the cavities of zeolite-Y during the encapsulation process via FL method. However, formation of some of the metal complexes can take place on the surface and some ligands molecules may remain un-coordinated as well. As stated ahead, zeolite-Y encapsulated complexes were Soxhlet extracted with 1,4-dioxane and acetonitrile to remove undesired molecules from the external surface. To ensure the surface morphology of the zeolite-Y after encapsulation process, SEM images of a representative [VO(pamp)-Y] catalyst were recorded. The SEM image of [VO(pamp)]-Y taken before Soxhlet extraction display the deposition of complexes on the peripheral surface. However, the absence of extraneous materials in the SEM

photographs after Soxhlet extraction specifies the complete removal of extraneous complexes from peripheral surface, leading to the presence of well-defined encapsulation in the cavity (see supplementary data) [46].

3.2.5 FTIR spectral study

To verify the presence of the complex in the zeolitic framework, the IR spectra of the neat and encapsulated complexes have been compared (Table 2). A sharp band is detected in zeolite-Y encapsulated complexes at $\sim 1070\text{cm}^{-1}$, which is missing in the ligand pamp and their neat complexes (Fig. 1). Therefore, it could be recognized to the asymmetric stretching vibrations of $(\text{SiO}_4/\text{AlO}_4)$ units [47]. The spectra of the neat and encapsulated complexes were matched with that of the ligand pamp to define the coordination sites which involved in chelation. The IR spectrum of the neat and encapsulated complexes shows a sharp band at $\sim 1615\text{cm}^{-1}$; which can be recognized by the vibration band of the azomethine group [48,49]. But the hybrid materials usually tend to absorb moisture, hence, this band in the case of $[\text{M}(\text{pamp})]\text{-Y}$ may overlap with the H–O–H bending band appearing in this region. The bending band of H_2O can be eliminated upon careful drying of the zeolite material. The $[\text{M}(\text{pamp})]\text{-Y}$ was heated in an air-oven at $120\text{ }^\circ\text{C}$ for two hours and was immediately dried in a vacuum desiccator, so that water cannot be absorbed. No band for zeolite-Y appears in this region. So, the appearance of a band at $\sim 1615\text{cm}^{-1}$ can be attributed to the azomethine vibration bands and it can be predicted that metal complex is really present in the matrix of zeolite-Y. In IR spectra of ligand, a sharp band is observed at $\sim 1315\text{cm}^{-1}$ attributed to aromatic -OH. However, in the case of neat and zeolite-Y encapsulated complexes, this band is completely missing, which proves the involvement of aromatic -OH in coordination with metal. The absorption band in the ligand at 1350cm^{-1} attributed to the phenolic oxygen (C–O) group was shifted to lower frequencies in all complexes. This indicates the contribution of the phenolic oxygen and azomethine nitrogen in metal-ligand coordination [50]. An important feature is the presence of new intense bands are observed in the far-IR region ($415\text{-}480\text{cm}^{-1}/403\text{-}414\text{cm}^{-1}$) in zeolite-Y encapsulated complexes assigned to $\nu_{(\text{M-O})}$ and $\nu_{(\text{M-N})}$, stretching vibrations, which confirms the coordination of oxygen and nitrogen atoms of the ligand to the metal atom.

A broad band in the region $3430\text{--}3449\text{cm}^{-1}$, and two weaker bands in the region $\sim 830\text{cm}^{-1}$ and $\sim 675\text{cm}^{-1}$ in all zeolite-Y encapsulated complexes are attributed to --OH stretching, rocking and wagging vibrations, respectively, of coordinated water molecules [51]. The symmetric stretching and bending bands of the Al–O–Si framework of the zeolite appears at $\sim 732\text{cm}^{-1}$ and 454cm^{-1} respectively, shows that the zeolite network remains intact [52,53]. However, in the spectra of zeolite-Y encapsulated complexes, low concentration of the complex within zeolite is responsible for the weak peak intensities [54]. IR data showed that the ligand is a tetradentate binegative ligand coordinating to the metal ion through two azomethine nitrogen and two deprotonated oxygen atoms.

3.2.6 Electronic spectral study

The electronic spectra of ligand pamp and neat complexes were recorded in methanol, while of zeolite-Y encapsulated complexes were taken in dilute HF solution. As tabulated in Table 4, electronic spectra of the ligand pamp show three bands at 228, 288 and 331 nm and these are assigned due to ILCT (intra-ligand charge transfer transition), $\pi\rightarrow\pi^*$ transition in phenyl ring and $n\rightarrow\pi^*$ transition of C=N chromophore, respectively. The values of the former two bands are comparable to the values for the neat complexes. Though, $n\rightarrow\pi^*$ transition has undergone hypsochromic shifts and appeared at higher wavelength viz., 401 nm in VO(IV), 532 nm in Mn(II), 363 nm in Fe(II) and 413 nm in Cu(II) neat complexes resulting from the chelation of the ligand with the transition metal ions. This value is exceptionally comparable to the values for the encapsulated complexes observed at ~ 471 nm.

The electronic spectra of neat VO(IV) complex consist three absorption bands in the region of 237 nm, 314 nm, and 401 nm confirms square pyramidal structure [55]. Mn(II) complex show intense absorption at 330 nm assigned to ligand centered transitions. The weak transition observed at 532 nm may be referred to d–d transition. The spectroscopic profile supports tetrahedral Mn^{2+} stereochemistry. The distorted tetrahedral geometry of Fe(II) is strongly indicated by similarities in the visible spectra with those of known tetrahedral complexes containing oxygen–nitrogen donor atoms [56]. The electronic spectra of Cu(II) complex exhibit four bands at 306, 340, 413, and 566 nm. The band at 566 nm in the electronic spectrum of the Cu(II) complex is indicative of a ${}^2B_{1g}\rightarrow{}^2A_{1g}$ which is in conformity to a square planar geometry [57]. All encapsulated complexes derived from

ligand pamp, possess basically similar spectral patterns with their respective neat complexes, which confirms the presence of complexes in the cavity of zeolite-Y (see supplementary data) [58].

3.2.7 Thermogravimetric (TG) analysis

The thermal behavior of the neat and zeolite-Y encapsulated complexes has been characterized (see supplementary data) on the basis of a thermogravimetric (TG) method to check the presence of water molecules in the coordination sphere of metal complexes and the existence of metal complexes in the cavity of zeolite-Y as well. As shown in Table 5, TGA profile of ligand pamp exhibits a mass loss of 36.41% at 140-160 °C, which may be recognized to the liberation of the first part of the ligand. In the second stage, remaining part loses within the temperature range 161-250 °C, with an estimated mass loss of 63.59%.

The thermal degradation of neat complexes takes place in two stages. The first decomposition stage is in the temperature range of ~30-500 °C, which is attributed to the loss of ligand pamp ($C_{20}H_{16}N_2O_2$), with the observed mass loss of ~70-90%. The final residues were estimated as metal oxides. The thermal decomposition of zeolite-Y encapsulated complexes usually undergoes in two stages. The removal of intrazeolite and coordinated water molecules follows in the temperature range of ~30-200 °C. The second step starts above 400 °C and continues to 700 °C, which involves the weight loss of ~8% due to the decomposition of metal complexes. Less fraction of weight loss specifies the existence of merely a small amount of metal complex within zeolitic voids.

3.3 Catalytic properties

With cyclohexanone as a typical substrate, the B-V oxidation was catalyzed by zeolite-Y encapsulated complexes in the presence of 30% H_2O_2 as an oxidant. In a typical reaction, 1:1 molar ratio of the cyclohexanone (0.01 mole) and 30% H_2O_2 (0.01 mole) were taken with 3 mL of acetonitrile, 30 mg of the catalyst was added to it and equilibrated at 70 °C in an oil-bath with continuous stirring for 12 h. The filtrate was collected at different time intervals and exposed to GC in order to identify the products.

The blank reactions performed over zeolite-Y under the same reaction conditions showed minor conversion specifying that host alone without the metal complexes is catalytically inactive. As shown in Fig. 2, neat complexes displayed some activity for B-V

oxidation of cyclohexanone, but both cyclohexanone conversion and ϵ -caprolactone selectivity were much less than the respective encapsulated complexes under identical conditions (Table 6). Additionally, heterogeneous catalyst [VO(pamp)]-Y showed higher activity by providing 967 TONs, hence, it was chosen as a representative catalyst to check the effect of experimental variables on cyclohexanone oxidation as described below.

3.3.1 Effect of solvents

In the present study, five different solvents were used with [VO(pamp)]-Y catalyst to see their effect on B-V oxidation of cyclohexanone (Fig. 3). The conversion percent and TONs obtained with different solvent decreases in the order, acetonitrile > 1,4-dioxane > 1,2-dichloroethane > methanol > n-butanol > chloroform. Acetonitrile shows higher TON though it is difficult to describe that which goods of the solvent influenced the cyclohexanone conversion. It may be possible that due to high polarity, it may readily dissolve H₂O₂ beside cyclohexanone and subsequently can direct the reactants in such a way that appropriately be adsorbed on the catalyst exterior and thereby boost the catalytic activity [59]. It has also been used in other cases as the most appropriate solvent for similar B-V oxidation reactions [60,61].

3.3.2 Effect of catalyst amount

The concentration of catalyst was crucial to the conversion of the heterogeneous catalyzed B-V oxidation of cyclohexanone. Values of TON are given in Fig. 4 for typical essays. Increasing the amount of [VO(pamp)]-Y catalyst results in higher TON, e.g. the TON enhances from 961 to 1115 upon changing that amount from 10 to 25 mg. However, the TON decreased by further raising the catalyst amount up to 30 mg. The increase in catalyst amount above 10 mg leads to increase in amount of the radical formation, where the rate of radical formation is higher compared to radical recombination. However, when amount of catalyst is large (above 25 mg), the rate of radical recombination becomes higher in comparison to radical formation. In this case, this change is observed when amount of catalyst is 25 mg. Therefore, 25 mg catalyst was sufficient to carry out the catalytic reactions.

3.3.3 Effect of molar ratio of substrate to oxidant

A series of reactions were carried out to investigate the consequences of the substrate to oxidant molar ratios on the B-V oxidation of cyclohexanone. Four different ratios of cyclohexanone to 30% H₂O₂ were used to investigate the corresponding variations of the oxidation results (Fig. 5). We steadied the substrate value and changed the amount of oxidant. Conversion of cyclohexanone was increased up to 37% with 1423 TONs upon increasing molar ratio up to 1:2. Further, rising in molar ratio results in low conversion and ϵ -caprolactone selectivity as well. It may be owing to the breakdown of H₂O₂ produces the additional water, which dilutes the reaction mixture thus dropping the conversion rate. Moreover, the presence of excess water may have also deactivated the catalyst. Hence, 1:2 molar ratio was chosen to be as optimized for B-V oxidation of cyclohexanone.

3.3.4 Effect of temperature with reaction time

To adjust the prime reaction temperature, catalytic B-V oxidation was examined at different temperature (Fig. 6). It can be seen that cyclohexanone conversion increased with a temperature rising and reached the top until 80 °C with 1500 TONs. However, the conversion was decreased with a temperature above 80 °C, owing to the decomposition of H₂O₂. Additionally, more than 12 h reaction time results in low selectivity of ϵ -caprolactone, viz., 90, 89, 89, 85.2, 84, 79, 71, and 64 % for 3, 6, 9, 12, 15, 18, 21, and 24 h reaction time, respectively (at 80 °C). It was due to the further hydrolysis of ϵ -caprolactone to hexanoic acid [62,63]. It meant that the reaction temperature was one of influencing factor for B-V oxidation of cyclohexanone, and the optimum temperature was 80 °C with 12 h reaction time.

3.4 Stability of catalysts

Homogeneous metal complexes as catalysts are more prone due to the formation of μ -oxo and μ -peroxo dimeric and other polymeric species, which is expected to be reduced by encapsulating them in zeolites. After optimization of reaction conditions, a series of reactions were performed to check the efficiency of [VO(pamp)]-Y catalyst on B-V oxidation of cyclohexanone (Table 7). Fresh [VO(pamp)]-Y catalyst has shown 39% conversion of cyclohexanone with 85.2% selectivity towards ϵ -caprolactone by providing 1500 TONs.

Furthermore, it was recycled and washed with acetonitrile after each run and dried at 120 °C for the B-V oxidation of cyclohexanone with a view to establishing the effect of encapsulation on thermal stability, catalytic activity, and reusability. Under the same reaction conditions, the catalytic activity in successive runs has no apparent reduction as compared to the fresh catalyst, providing 1466, 1458, and 1451 TONs for three consecutive runs, respectively. Moreover, the atomic absorption spectroscopic analysis did not show any vanadium metal content in the filtrate, which validates that vanadium is not leaching out from the catalyst during B-V oxidation reaction. Hence, it is flawless to say that the porous support prevents the complex from dimerization and decomposition during the reaction, and makes it recyclable and reusable.

Catalytic B-V oxidation of cyclohexanone by an assortment of groups through varied homogeneous and/or heterogeneous systems has been discussed. Q. Ma et al. (Table 8, entry 1) reported B-V oxidation of cyclic ketones catalyzed by transition metal oxides viz., MoO₃, WO₃, TiO₂, Fe₂O₃, Co₃O₄, ZnO and ZrO₂ using aqueous hydrogen peroxide. About 92% conversion of cyclohexanone was observed with MoO₃, however, the selectivity of ϵ -caprolactone was only 22% [64]. S. Baj et al. (Table 8, entry 2) carried out oxidation of cyclohexanone over acidic ionic liquid [hmim][AlxCl_y] using (Me₃SiO₂)₂ as oxidant results in 60% conversion with 55% yield of ϵ -caprolactone [11]. Fe(III) picolinate and Fe(III) dipicolinate complexes were immobilized on to kaolinite furnished heterogeneous catalysts by E.H. de Faria et al. (Table 8, entry 3). As prepared catalysts were effective in cyclohexanone oxidation with 60% substrate conversion and 100% selectivity for ϵ -caprolactone [65]. A. Corma (Table 8, entry 4) described a new heterogeneous catalyst, Sn-MCM-41, providing 97% selectivity of ϵ -caprolactone. Though, conversion and TONs were low [66]. B-V oxidation of cyclohexanone have been done by Z. Lei et al. (Table 8, entry 5) with Sn-palygorskite catalyst in the presence of H₂O₂, affording 90-100% lactones or esters selectivity. However, they also faced low conversion and TONs as well [67]. A.J.L. Pombeiro and coworkers (Table 8, entry 6) tested [ReO₃{ κ^2 -HC(pz)₃}(PTA)][ReO₄] catalyst in the oxidation of cyclohexanone in the presence of aqueous H₂O₂, allowing to achieve 38% conversion and 26% ϵ -caprolactone selectivity [12]. Sn-doped hydrotalcite (Sn/HT) (Table 8, entry 7) have been found to be an efficient catalyst for the liquid phase B-V oxidation of cyclohexanone to the corresponding lactone by providing 119 TONs in the presence of H₂O₂

in acetonitrile solvent [68]. Z. Lei, et al. (Table 8, entry 8) have reported B-V oxidation of cyclohexanone by Montmorillonite supported SnCl_2 catalyst resulted in 100% conversion with 100% ϵ -caprolactone selectivity though TONs was only 166 [69]. E.C.B.A. Alegria et al. tested $[\text{ReCl}_2\{\eta^2\text{-}N,O\text{-}C(\text{O})\text{Ph}\}(\text{PPh}_3)_2]$ as a homogeneous catalyst for the oxidation of cyclohexanone (Table 8, entry 9) resulted in 57% conversion and 30% ϵ -caprolactone selectivity [13]. B. Dutta et al. (Table 8, entry 10) obtained a good selectivity of ϵ -caprolactone by using zeolite-Y immobilized complex $\text{Sn}(\text{salen})\text{-NaY}$ (1210 TONs) as a heterogeneous catalyst [38].

3.5 Catalytic mechanism

As shown in Scheme 2, the probable mechanism for B-V oxidation of cyclohexanone using $[\text{VO}(\text{pamp})]\text{-Y}$ catalyst in the presence of H_2O_2 oxidant is proposed. From UV-Vis spectra and TGA data, it can be decided that $[\text{VO}(\text{pamp})]\text{-Y}$ (**A** in Scheme 2) catalyst has a square pyramidal geometry in the zeolite framework. The ligand pamp may perhaps stay on the coordination sites of the equatorial positions (parallel with respect to metal) while oxygen atom settle in the axial positions (perpendicular with respect to metal). The first step involves the activation of carbonyl group of the ketone by the coordination to the Lewis-acid vanadium (**B** in Scheme 1) [70,71], thereby increasing the nucleophilic attack of H_2O_2 on the carbonyl carbon to give an intermediate (**C** in Scheme 2) alike to the Criegee adduct, which rearranges to the ϵ -caprolactone (**D** in Scheme 2), and desorbed from the zeolite-Y by a fresh cyclohexanone moiety. Even though the conversion was not too upright and the selectivity for ϵ -caprolactone was bit poor as well, which was ascribed to zeolitic acid sites favoring opening of the lactone ring, led to the formation of 6-hydroxyhexanoic acid [72,73].

4. Conclusions

- ✚ Encapsulation of metal complexes inside the zeolite-Y framework was successfully done by the FL method as verified by various characterization techniques viz., chemical analysis, BET, UV-Vis, IR, powder XRD, SEM, and TGA.
- ✚ B-V oxidation of cyclohexanone was catalyzed in both the homogeneous and heterogeneous systems by using neat and zeolite-Y encapsulated complexes, respectively.

- ✚ Factors that affect the B-V oxidation (solvents, catalyst amount, the molar ratio of substrate to oxidant, temperature, and reaction time) were also thoroughly checked and the reaction conditions were improved as 0.01 mole cyclohexanone, 0.02 mole 30% H₂O₂, 25 mg [VO(pamp)]-Y, 3 mL acetonitrile, 80 °C, 12 h.
- ✚ [VO(pamp)]-Y showed concluding performance by providing 1500 TONs (39% cyclohexanone conversion; 85.2% ε-caprolactone selectivity) that will go up in the innovative research.
- ✚ Therefore, heterogeneous catalysis will be more than pleased with the plenty of advantages over homogeneous as it is looked-for the handling, separation and recycling abilities from an economical, technical and environmental point of view.

Acknowledgements

One of the authors Digvijaysinh K. Parmar is thankful to UGC, New Delhi for providing partial financial assistant (JRF) for this work.

References

- [1] M. Renz, B. Meunier, *Eur. J. Org. Chem.* 4 (1999) 737-750.
- [2] G.J. ten Brink, I.W.C.E. Arends, R.A. Sheldon, *Chem. Rev.* 104 (2004) 4105-4123.
- [3] S. Xu, Z. Wang, X. Zhang, X. Zhang, K. Ding, *Angew. Chem. Int. Ed.* 47 (2008) 2840-2843.
- [4] Y.F. Li, M.Q. Guo, S.F. Yin, L. Chen, Y.B. Zhou, R.H. Qiu, C.T. Au, *Carbon* 55 (2013) 269-275.
- [5] A. Corma, L.T. Nemeth, M. Renz, S. Valencia, *Nature* 412 (2001) 423-425.
- [6] G.J. ten Brink, I.W.C.E. Arends, R.A. Sheldon, *Chem. Rev.* 104 (2004) 4105-4123.
- [7] J. Muzart, *Adv. Synth. Catal.* 348 (2006) 275-295.
- [8] W.F. Sager, A. Duckworth, *J. Am. Chem. Soc.* 77 (1955) 188-190.
- [9] N. Friess, N. Famham, *J. Am. Chem. Soc.* 72 (1950) 5518-5521.
- [10] G.R. Krow, in: B.M. Trost, I. Fleming (Eds.), *Comprehensive Organic Synthesis*, Pergamon Press, New York, 1991.
- [11] S. Baj, R. Słupska, A. Chrobok, A. Drożdż, *J. Mol. Catal. A: Chem.* 376 (2013) 120-126.
- [12] L.M.D.R.S. Martins, E.C.B.A. Alegria, P. Smoleński, M.L. Kuznetsov, A.J.L. Pombeiro, *Inorg. Chem.* 52 (2013) 4534-4546.
- [13] E.C.B.A. Alegria, L.M.D.R.S. Martins, M.V. Kirillova, A.J.L. Pombeiro, *Appl. Catal. A: Gen* 443-444 (2012) 27-32.
- [14] Q.H. Fan, Y.M. Li, A.C. Chan, *Recoverable Catalysts for Asymmetric Organic Synthesis*, Chemical review Rev, American Chemical Society, 2002, pp. 3385-3466.
- [15] L. Saikia, D. Srinivas, P. Ratnasamy, *Appl. Catal. A: Gen* 309 (2006) 144-154.
- [16] C. Schuster, W.F. Hölderich, *Catal. Today* 60 (2000) 193-207.
- [17] A.A. Valente, J. Vital, *J. Mol. Catal. A: Chem.* 156 (2000) 163-172.
- [18] W.F. Hölderich, *Catal. Today* 62 (2000) 115-130.
- [19] J. Pires, J. Francisco, A. Carvalho, M. Brotas de Carvalho, A.R. Silva, C. Freire, B. de Castro, *Langmuir* 20 (2004) 2861-2866.
- [20] V.K. Bansal, P.P. Thankachan, R. Prasad, *Appl. Catal. A: Gen.* 381 (2010) 8-17.
- [21] C.K. Modi, P.M. Trivedi, *Micropor. Mesopor. Mat.* 155 (2012) 227-232.
- [22] M.R. Maurya, P. Saini, C. Haldar, F. Avecilla, *Polyhedron* 31 (2012) 710-720.
- [23] A. Choudhary, B. Das, S. Ray, *Dalton Trans.* 44 (2015) 3753-3763.

- [24] N. Herron, *Chem. Technol.* 19 (1989) 542-548.
- [25] K. Kervinen, C.A.B. Pieter, M.B. Andrew, J.G. Gerbrand Mesu, G. Koten, J.M.K.G. Robertus, B.M. Weckhuysen, *J. Am. Chem. Soc.* 128 (2006) 3208-3217.
- [26] C.K. Modi, P.M. Trivedi, S.K. Gupta, P.K. Jha, *J. Incl. Phenom. Macrocycl. Chem.* 74 (2012) 117-127.
- [27] K.K. Bania, D. Bharali, B. Viswanathan, R.C. Deka, *Inorg. Chem.* 51 (2012) 1657-1674.
- [28] A. Corma, H. Garcia, *Eur. J. Inorg. Chem.* 6 (2004) 1143-1164.
- [29] R.F. Parton, L. Uytterhoeven, P.A. Jacobs, *Stud. Surf. Sci. Catal.* 59 (1991) 395-403.
- [30] R. Grommen, P. Manikandan, Y. Gao, T. Shane, J.J. Shane, R.A. Schoonheydt, B.M. Weckhuysen, D. Goldfarb, *J. Am. Chem. Soc.* 122 (2000) 11488-11496.
- [31] K.K. Bania, R.C. Deka, *J. Phys. Chem. C* 115 (2011) 9601-9607.
- [32] M. Salavati-Niasari, M. Shakouri-Arani, F. Davar, *Micropor. Mesopor. Mat.* 116 (2008) 77-85
- [33] M.R. Maurya, A.K. Chandrakar, S. Chand, *J. Mol. Catal. A: Chem.* 270 (2007) 225-235.
- [34] I.K.-Biernacka, A.M. Fonseca, I.C. Neves, *Inorg. Chim. Acta* 394 (2013) 591-597.
- [35] V.K. Bansal, P.P. Thankachan, R. Prasad, *Appl. Catal. A: Gen* 381 (2010) 8-17.
- [36] M. Salavati-Niasari, *J. Incl. Phenom. Macrocycl. Chem.* 65 (2009) 349-360.
- [37] M. Madadi, R. Rahimi, *Reac. Kinet. Mech. Cat.* 107 (2012) 215-229.
- [38] B. Dutta, S. Jana, S. Bhunia, H. Honda, S. Koner, *Appl. Catal. A: Gen* 382 (2010) 90-98
- [39] T. Kawabata, Y. Ohishi, S. Itsuki, N. Fujisaki, T. Shishido, K. Takaki, Q.H. Zhang, Y. Wang, K. Takehira, *J. Mol. Catal. A: Chem.* 236 (2005) 99-106.
- [40] M.B. Gholivand, F. Ahmadi, E. Rafiee, *Separ. Sci. Technol.* 41 (2006) 315.
- [41] C.K. Modi, P.M. Trivedi, *Micropor. Mesopor. Mat.* 155 (2012) 227-232.
- [42] A. Corma, H. Garcia, *Eur. J. Inorg. Chem.* 6 (2004) 1143-1164.
- [43] W. H. Quayle, J. H. Lunsford, *Inorg. Chem.*, 1982, 21, 97-103.
- [44] W. H. Quayle, G. Peeters, G. L. De Roy, E. F. Vansant, J. H. Lunsford, *Inorg. Chem.*, 1982, 21, 2226-2231.
- [45] M. Jafarian, M. Rashvandavei, M. Khakali, F. Gobal, S. Rayati, M. G. Mahjani, *J. Phys. Chem. C*, 2012, 116, 18518-18532.
- [46] K. K. Bania, D. Bharali, B. Viswanathan, R. C. Deka, *Inorg. Chem.*, 2012, 51, 1657-1674.
- [47] V. Arun, N. Sridevi, P.P. Robinson, S. Manju, K.K.M. Yusuff, *J. Mol. Catal. A: Chem.* 304 (2009) 191-198.

- [48] R.M. Silverstein, G.C. Bassler, *Spectrometric Identification of Organic Compounds*, John Wiley and Sons Inc., New York, 1963.
- [49] S. Das, S. Pal, *J. Organomet. Chem.* 691 (2006) 2575-2583.
- [50] K. Nakamoto, *Infrared Spectra of Inorganic and Coordination Compounds*, Wiley Interscience, New York, 1970.
- [51] K. Nakamoto, *Infrared Spectra and Raman Spectra of Inorganic and Coordination Compounds, Part B: Application in Coordination, Organometallic, and Bioinorganic Chemistry*, sixth ed., Wiley Interscience, New Jersey, 2009.
- [52] D.K. Dey, M.K. Das, H. Nöth, *Z. Naturforsch.* 54b (1999) 145-154.
- [53] R.M. Barrer, *Hydrothermal Chemistry of Zeolites*, Academic Press, New York, 1982.
- [54] M.J. Alcón, A. Corma, M. Iglesias, F. Sánchez, *J. Mol. Catal. A: Chem.* 194 (2003) 137-152.
- [55] S. Bertini, A. Coletti, B. Floris, V. Conte, P. Galloni, *J. Inorg. Biochem.* 147 (2015) 44–53.
- [56] A.V. Wiznycia, J. Desper, C.J. Levy, *Chem. Commun.* (2005) 4693–4695.
- [57] N. Raman, V. Muthuraj, S. Ravichandran, A. Kulandaisamy, *J. Chem. Sci.* 115 (2003) 161-167.
- [58] B. Fan, W. Fan, R. Li, *J. Mol. Catal. A: Chem.* 201 (2003) 137-144.
- [59] M. Salavati-Niasari, *Inorg. Chim. Acta* 362 (2009) 2159-2166.
- [60] H. Xu, J. Jiang, B. Yang, H. Wu, P. Wu, *Catal. Commun.* 55 (2014) 83-86.
- [61] H.J. Xu, F.F. Zhu, Y.Y. Shen, X. Wan, Y.S. Feng, *Tetrahedron* 68 (2012) 4145-4151.
- [62] A.R. Olson, J.L. Hyde, *J. Am. Chem. Soc.* 63 (1941) 2459-2461.
- [63] M. Lenarda, M. Da Ros, M. Casagrande, L. Storaro, R. Ganzerla, *Inorg. Chim. Acta* 349 (2003) 195-202.
- [64] Q. Ma, W. Xing, J. Xu, X.Peng, *Catal. Commun.* 53 (2014) 5-8.
- [65] E.H. de Faria, G.P. Ricci, L. Marc, E.J. Nassar, M.A. Vicente, R. Trujillano, A. Gil, S.A. Korili, K.J. Ciuffi, P.S. Calefi, *Catal. Today* 187 (2012) 135-149.
- [66] A. Corma, M.T. Navarro, L. Nemeth, M. Renz, *Chem. Commun.* (2001) 2190-2191.
- [67] Z. Lei, Q. Zhang, J. Luo, X. He, *Tetrahedron Lett.* 46 (2005) 3505-3508.
- [68] U.R. Pillai, E. Sahle-Demessie, *J. Mol. Catal. A: Chem.* 191 (2003) 93-100.
- [69] Z. Lei, G. Ma, C. Jian, *Catal. Commun.* 8 (2007) 305-309.
- [70] A. Corma, L.T. Nemeth, M. Renz, S. Valencia, *Nature* 412 (2001) 423–425.
- [71] R. Ganesan, B. Viswanathan, *J. Phys. Chem. B* 108 (2004) 7102-7114.

- [72] M. Lenarda, M. Da Ros, M. Casagrande, L. Storaro, R. Ganzerla, *Inorg. Chim. Acta* 349 (2003) 195-202.
- [73] C. J-Sanchidria'n, J.R. Ruiz, *Tetrahedron* 64 (2008) 2011-2026.

Table 1.

Compound	Elements found (%)							
	C	H	N	M	C/N	Si	Al	Si/Al
Na-Y	-	-	-	-	-	17.16	6.60	2.60
VO(IV)-Y	-	-	-	5.86	-	16.84	6.47	2.60
Mn(II)-Y	-	-	-	5.74	-	16.30	6.25	2.60
Fe(II)-Y	-	-	-	6.85	-	16.62	6.39	2.60
Cu(II)-Y	-	-	-	6.24	-	16.13	6.21	2.60
pamp	75.91 (75.93)	5.03 (5.10)	8.85 (8.86)	-	8.57 (8.56)	-	-	-
[VO(pamp)]	60.04 (63.00)	3.89 (3.70)	6.99 (7.35)	12.42 (13.36)	8.58 (8.57)	-	-	-
[Mn(pamp)]	59.20 (65.05)	4.21 (3.82)	6.89 (7.59)	13.11 (14.88)	8.56 (8.57)	-	-	-
[Fe(pamp)]	59.01 (64.89)	4.36 (3.81)	6.87 (7.57)	13.32 (15.09)	8.58 (8.57)	-	-	-
[Cu(pamp)]	63.60 (63.57)	4.18 (3.73)	7.40 (7.41)	16.26 (16.82)	8.59 (8.57)	-	-	-
[VO(pamp)]-Y	3.00	0.85	0.37	0.53	8.24	15.02	5.75	2.61
[Mn(pamp)]-Y	2.05	0.97	0.24	0.82	8.33	15.60	6.01	2.59
[Fe(pamp)]-Y	2.63	0.83	0.32	0.72	8.40	15.71	6.00	2.61
[Cu(pamp)]-Y	2.79	0.87	0.34	0.67	8.32	15.69	6.05	2.59

*% found (Calculated).

Table 2.

Compound	Internal vibrations			External vibrations			V _(C=N)	V _(O-H)	V _(C-O)
	V _{asym}	V _{sym}	V _{bend}		V _{sym}	V _{asym}			
	T-O	T-O	T-O	D-R	T-O	T-O			
pamp	-	-	-	-	-	-	1635	3405	1350
[VO(pamp)]	-	-	-	-	-	-	1608	3056	1317
[Mn(pamp)]	-	-	-	-	-	-	1614	3053	1276
[Fe(pamp)]	-	-	-	-	-	-	1608	3059	1319
[Cu(pamp)]	-	-	-	-	-	-	1608	3072	1328
[VO(pamp)]-Y	1072	678	459	607	831	1174	1614	3471	1335
[Mn(pamp)]-Y	1074	675	459	607	831	1176	1627	3439	1323
[Fe(pamp)]-Y	1072	680	459	607	831	1172	1618	3445	1340
[Cu(pamp)]-Y	1070	666	457	607	829	1174	1610	3500	1317

Table 3.

Compound	Specific surface area (m ² /g)	Specific pore volume (cm ³ /g)
Na-Y	630	0.320
V(IV)-Y	559	0.282
Mn(II)-Y	552	0.267
Fe(II)-Y	562	0.254
Cu(II)-Y	548	0.240
[VO(pamp)]-Y	358	0.162
[Mn(pamp)]-Y	365	0.170
[Fe(pamp)]-Y	342	0.135
[Cu(pamp)]-Y	332	0.131

Table 4.

Compound	Wavelength (nm)
pamp	228, 288, 331
[VO(pamp)]	237, 314, 401
[Mn(pamp)]	288, 330, 532, 588, 623, 975
[Fe(pamp)]	238, 263, 289, 363
[Cu(pamp)]	306, 340, 413, 566
[VO(pamp)]-Y	306, 395, 471, 501, 542, 968
[Mn(pamp)]-Y	276, 306, 473, 503, 540
[Fe(pamp)]-Y	270, 306, 314, 502, 542
[Cu(pamp)]-Y	256, 306, 471, 498, 543

Table 5.

Compound	TG range (°C)	Observed mass loss (%) (calc.)	Assignment
pamp	140-160	37.10	Removal of C ₇ H ₆ ON– part
	161-250	62.90	Removal of –C ₁₃ H ₁₁ NO part
[VO(pamp)]	30-520	83.86	Removal of ligand
	521-700	3.22	V ₂ O ₃ as residue
[Mn(pamp)]	30-630	97.62	Removal of ligand
	631-70	1.67	MnO ₂ as residue
[Fe(pamp)]	30-480	79.65	Removal of ligand
	481-700	19.61	Fe ₂ O ₃ as residue
[Cu(pamp)]	30-550	78.21	Removal of ligand
	551-700	11.58	CuO as residue
[VO(pamp)]-Y	50-200	11.29	Loss of crystallization H ₂ O
	401-700	8.07	Decomposition of complex
[Mn(pamp)]-Y	50-200	14.57	Loss of intrazeolite + coordinated H ₂ O
	401-700	6.91	Decomposition of complex
[Fe(pamp)]-Y	50-200	14.26	Loss of intrazeolite + coordinated H ₂ O
	401-700	7.24	Decomposition of complex
[Cu(pamp)]-Y	50-200	13.81	Loss of intrazeolite H ₂ O
	401-700	8.26	Decomposition of complex

Table 6.

Compound	Conversion (%)	TON ^b	TOF (h ⁻¹) ^c	ϵ -caprolactone selectivity (%)
Na-Y	1.3	-	-	-
VO(IV)-Y	4.3	-	-	25.0
Mn(II)-Y	3.5	-	-	17.3
Fe(II)-Y	3.9	-	-	24.5
Cu(II)-Y	4.0	-	-	27.0
[VO(pamp)]	17.2	24	2	60.2
[Mn(pamp)]	9.1	13	1.08	41.3
[Fe(pamp)]	10.0	14	1.16	58.0
[Cu(pamp)]	15.4	20	1.66	63.0
[VO(pamp)]-Y	30.2	967	80.58	88.0
[Mn(pamp)]-Y	19.0	424	35.33	73.0
[Fe(pamp)]-Y	19.3	500	41.66	85.0
[Cu(pamp)]-Y	21.9	693	57.75	90.0

^a Reaction conditions: 0.01 mole cyclohexanone, 0.01 mole 30% H₂O₂, 30 mg catalyst, 3 mL acetonitrile, 70 °C, 12 h.

^b TON: Turnover number (moles of cyclohexanone converted / mole of metal).

^c TOF: Turnover frequency (moles of cyclohexanone converted / mole of metal \times hour).

Table 7.

Catalyst	Conversion (%)	TON ^b	TOF (h ⁻¹) ^c	ϵ -caprolactone selectivity (%)
Fresh [VO(pamp)]-Y	39.0	1500	125	85.2 ^d
1 st run	38.1	1466	122.2	85.0
2 nd run	37.9	1458	121.5	84.7
3 rd run	37.7	1451	120.9	84.7

^a Reaction conditions: 0.01 mole cyclohexanone, 0.02 mole 30% H₂O₂, 25 mg [VO(pamp)]-Y, 3 mL acetonitrile, 80 °C, 12 h.

^b TON: Turnover number (moles of cyclohexanone converted / mole of metal).

^c TOF: Turnover frequency (moles of cyclohexanone converted / mole of metal × hour).

^d Remaining product is 6-hydroxyhexanoic acid.

Table 8.

Entry	Catalyst	Type of catalytic system	Cyclohexanone conversion (%)	TON ^a	TOF (h ⁻¹) ^b	ϵ -caprolactone selectivity (%)	Reference
1	MoO ₃	Homogeneous	92	-	-	22	60
2	[hmim][AlxCl _y]	Homogeneous	60	-	-	55	11
3	Fe(Ka-pa)-3	Heterogeneous	60	-	-	100	62
4	Sn-MCM-41(9% SnO ₂)	Heterogeneous	36	12	7	97	63
5	Sn-palygorskite	Heterogeneous	16	26	1	90	64
6	[ReO ₃ { κ^2 -HC(pz) ₃ }(PTA)][ReO ₄]	Homogeneous	38	102	17	26	12
7	Sn-doped hydrotalcite	Heterogeneous	30	119	30	>95	66
8	Montmorillonite supported SnCl ₂	Heterogeneous	100	166	7	100	67
9	[ReCl ₂ { η^2 -N,O-C(O)Ph}(PPh ₃) ₂]	Homogeneous	57	172	29	30	13
10	Sn(salen)-NaY	Heterogeneous	75	1210	50	90	38
11	[VO(pamp)]-Y	Heterogeneous	39	1500	125	85.20	Present work

^aTON: Turnover number (moles of cyclohexanone converted / mole of metal).

^bTOF: Turnover frequency (moles of cyclohexanone converted / mole of metal \times hour).

Fig. 1.

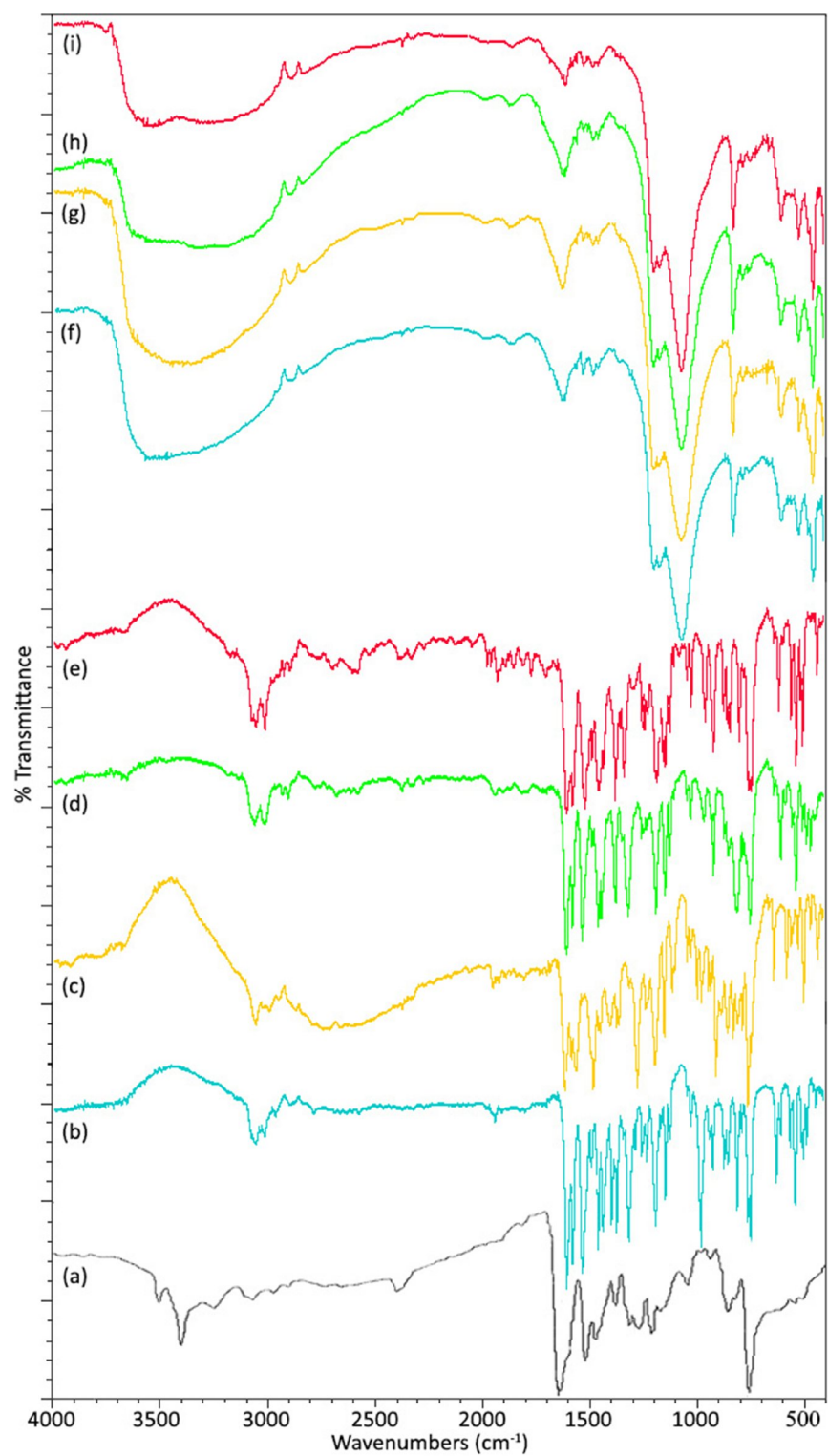
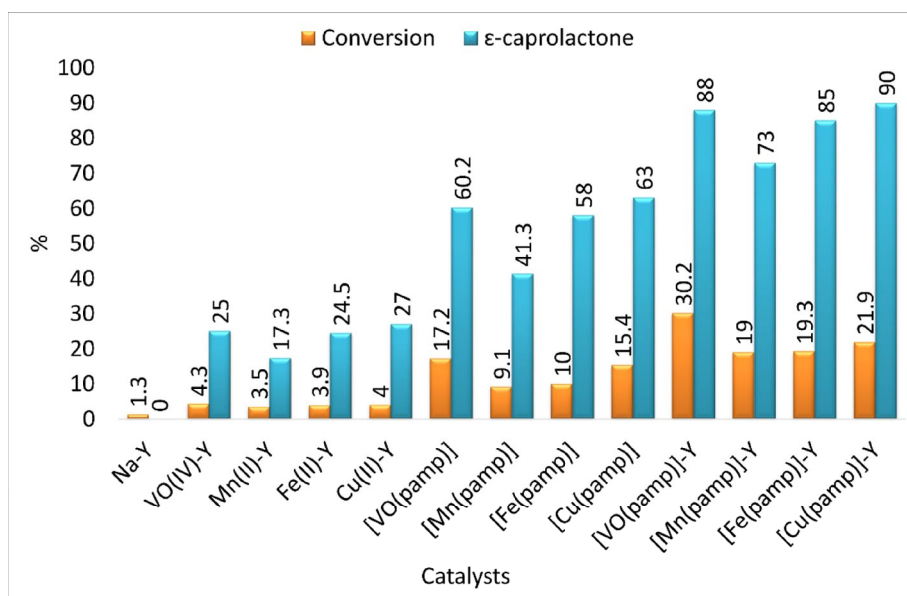
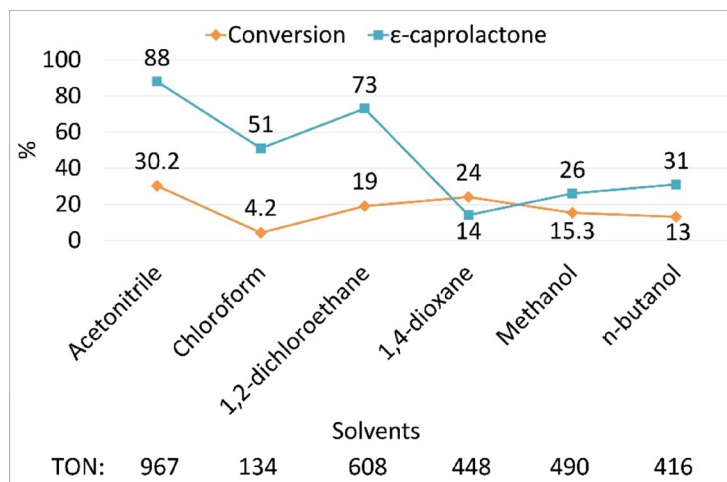


Fig. 2.



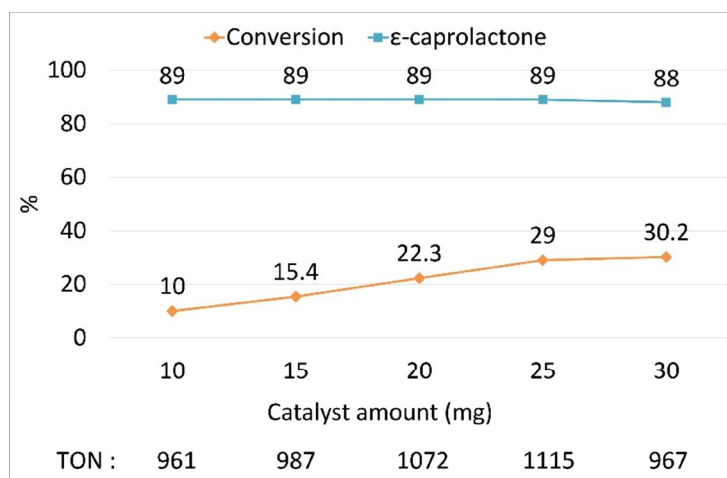
^a Reaction conditions: 0.01 mole cyclohexanone, 0.01 mole 30% H₂O₂, 30 mg catalyst, 3 mL acetonitrile, 70 °C, 12 h.

Fig. 3.



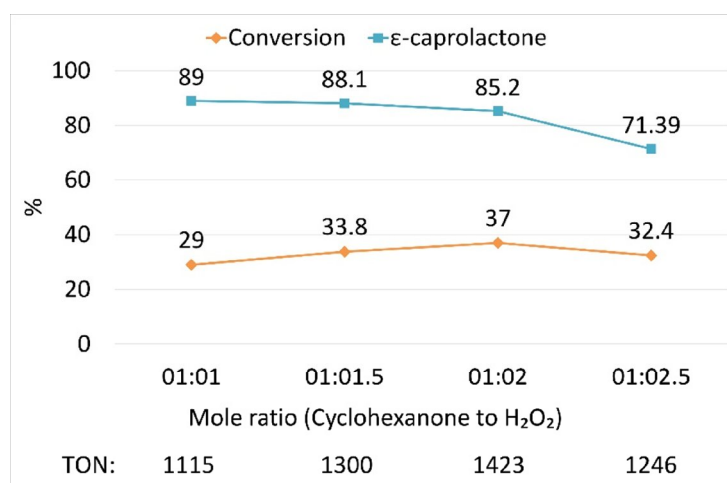
^a Reaction conditions: 0.01 mole cyclohexanone, 0.01 mole 30% H₂O₂, 30 mg [VO(pamp)]-Y, 3 mL X solvent, 70 °C, 12 h.

Fig. 4.



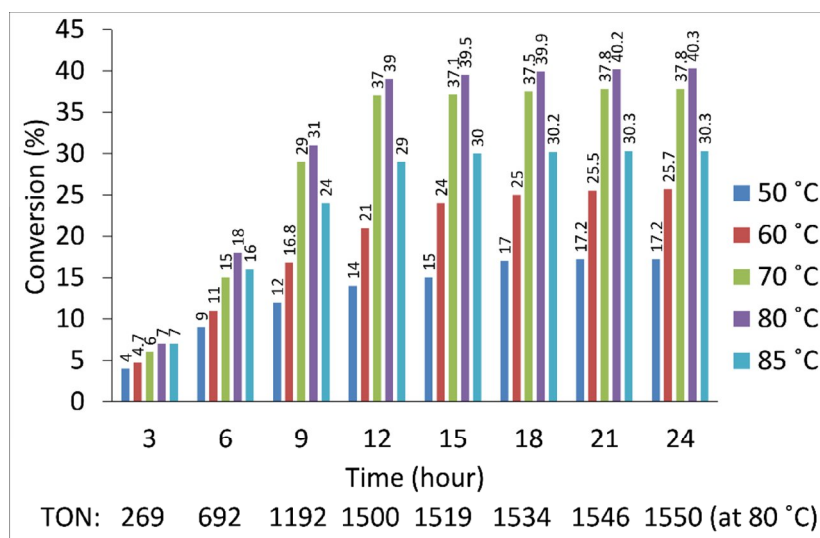
^a Reaction conditions: 0.01 mole cyclohexanone, 0.01 mole 30% H₂O₂, X mg [VO(pamp)]-Y, 3 mL acetonitrile, 70 °C, 12 h.

Fig. 5.

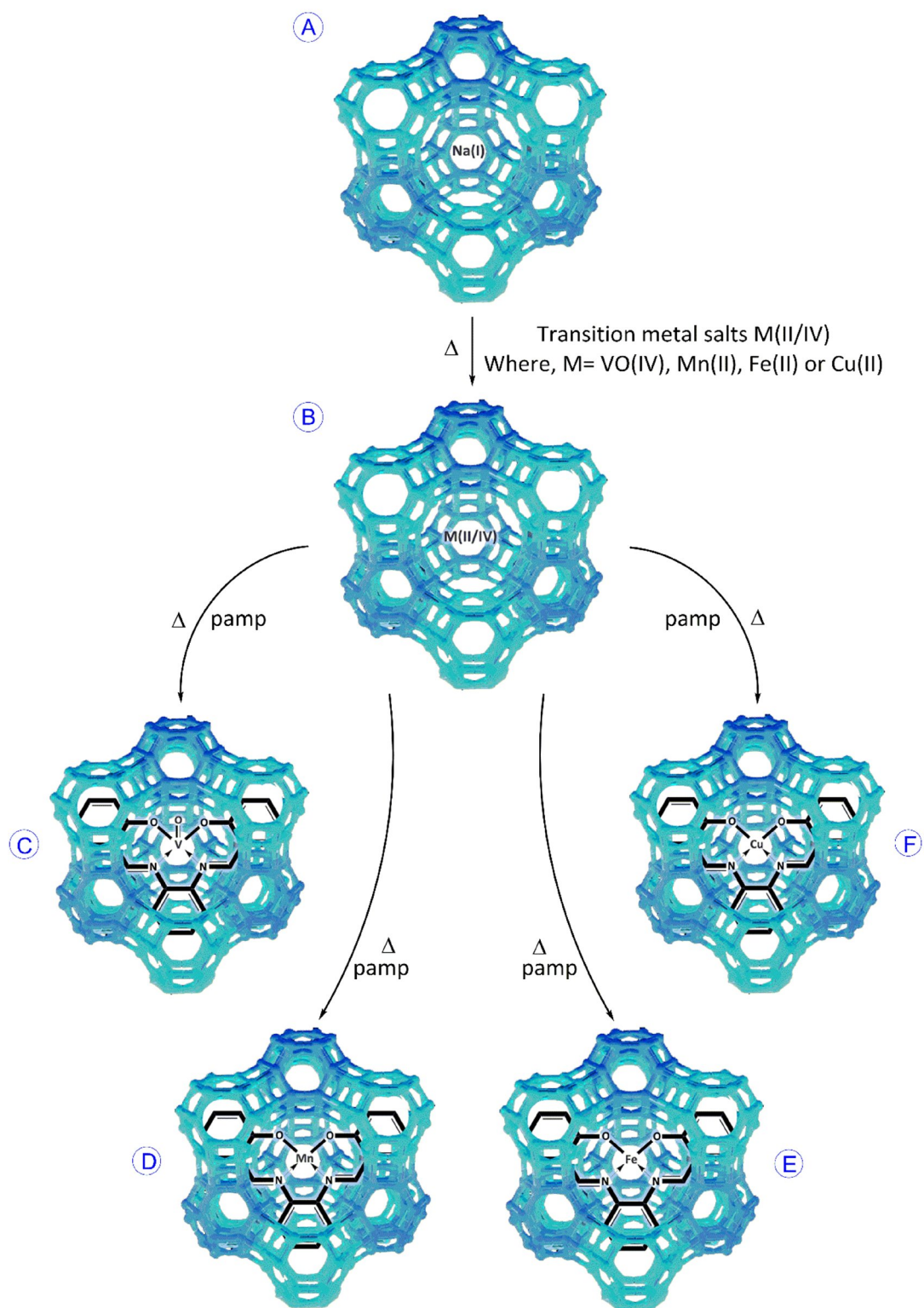


Reaction conditions: 0.01 mole cyclohexanone, X mole 30% H₂O₂, 25 mg [VO(pamp)]-Y, 3 mL acetonitrile, 70 °C, 12 h.

Fig. 6.

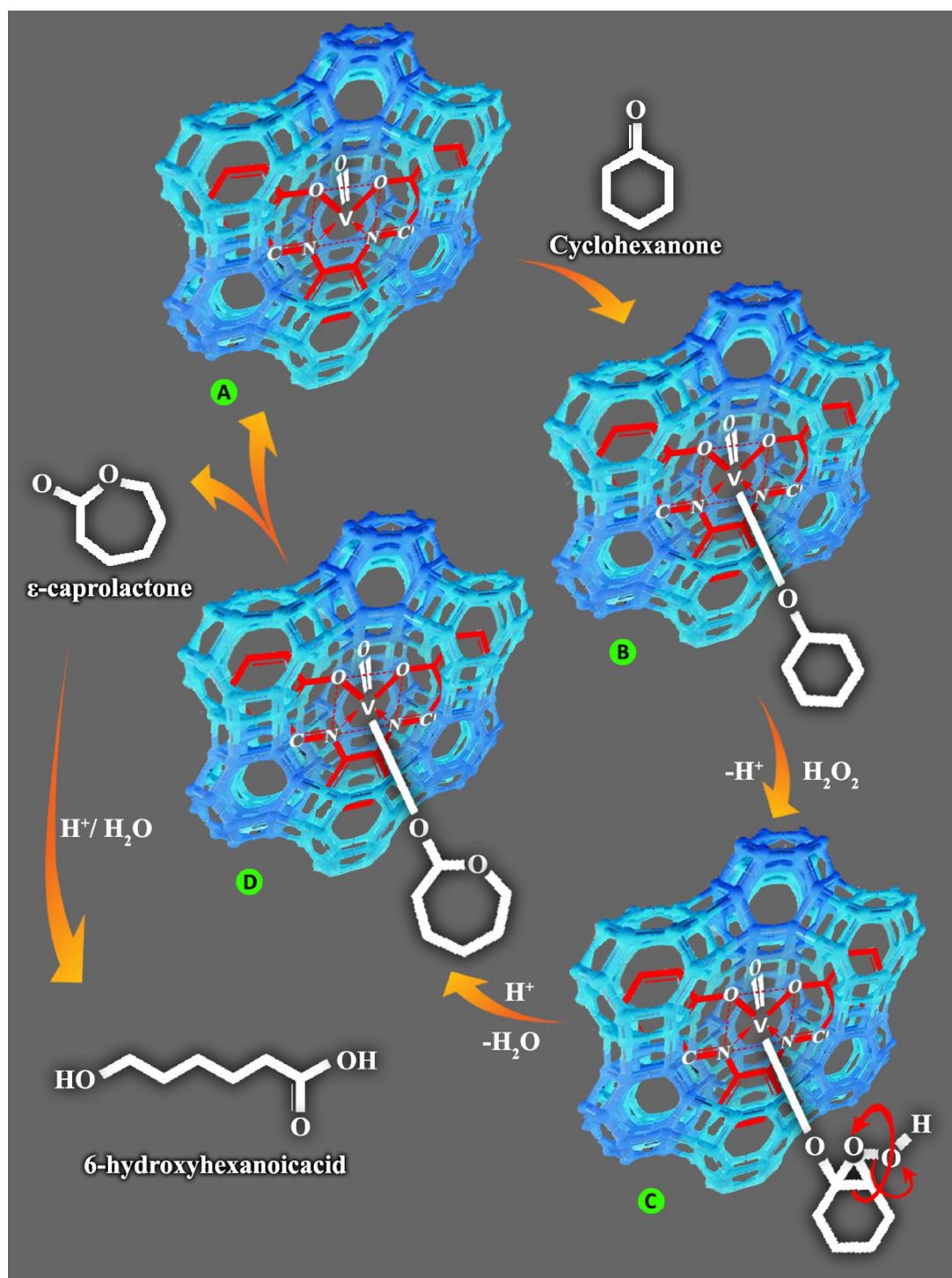


^a Reaction conditions: 0.01 mole cyclohexanone, 0.02 mole 30% H₂O₂, 25 mg [VO(pamp)]-Y, 3 mL acetonitrile, X °C, X h.



Where, (A) = Zeolite-Y
 (B) = Metal exchanged zeolite-Y
 (C) (D) (E) (F) = Zeolite-Y encapsulated complexes

Scheme 1.



Scheme 2.

Captions:

Table 1. The chemical composition of parent zeolite-Y, metal exchanged zeolite-Y, Schiff base ligand, neat complexes* and zeolite-Y encapsulated complexes.

Table 2. FT-IR data of Schiff base ligand, neat complexes and zeolite-Y encapsulated complexes.

Table 3. Specific surface area and pore volume data.

Table 4. Electronic spectral data of Schiff base ligand, neat complexes, and zeolite-Y encapsulated complexes.

Table 5. Thermogravimetric data of neat and zeolite-Y encapsulated complexes.

Table 6. Catalytic performance of synthesized materials over B-V oxidation of cyclohexanone^a.

Table 7. The outcome of recovered catalyst on the oxidation of cyclohexanone^a.

Table 8. Comparison between reported homogeneous and/or heterogeneous catalytic systems and our catalyst for B-V oxidation of cyclohexanone.

Fig. 1. FTIR spectra of (a) pamp, (b) [VO(pamp)] (c) [Mn(pamp)], (d) [Fe(pamp)], (e) [Cu(pamp)], (f) [VO(pamp)]-Y, (g) [Mn(pamp)]-Y, (h) [Fe(pamp)]-Y, and (i) [Cu(pamp)]-Y.

Fig. 2. B-V oxidation of cyclohexanone to ϵ -caprolactone with different catalysts^a.

Fig. 3. Effect of solvents on B-V oxidation of cyclohexanone^a.

Fig. 4. Effect of catalyst amount on B-V oxidation of cyclohexanone^a.

Fig. 5. Effect of molar ratio of cyclohexanone to 30% H₂O₂ on B-V oxidation of cyclohexanone^a.

Fig. 6. Effect of temperature with reaction time on B-V oxidation of cyclohexanone^a.

Scheme 1. Systematic synthetic pathway for the encapsulation of transition metal complexes inside the nanocavities of zeolite-Y via FL method.

Scheme 2. The probable mechanism for B-V oxidation of cyclohexanone using [VO(pamp)]-Y catalyst in the presence of 30% H₂O₂.